ISSN 1392–1320 MATERIALS SCIENCE (MEDŽIAGOTYRA). Vol. 19, No. 3. 2013

Plasma Deposition and Characterization of Copper-doped Cobalt Oxide Nanocatalysts

Ryszard KAPICA [1], Wiktor REDZYNIA [1], Marcin KOZANECKI [2], Mohamed M. CHEHIMI [3], Jan SIELSKI [1], Sławomir M. KUBERSKI [1], Jacek TYCZKOWSKI [1]*

[1] *Division of Molecular Engineering, Faculty of Process and Environmental Engineering, Lodz University of Technology, Wolczanska 213, 90-924 Lodz, Poland*
[2] *Department of Molecular Physics, Faculty of Chemistry, Lodz University of Technology, Zeromskiego 116, 90-924 Lodz, Poland*
[3] *Université Paris Diderot, Sorbonne Paris Cité, ITODYS, UMR CNRS 7086, 15 rue J-A de Baïf, 75013 Paris, France*

crossref http://dx.doi.org/10.5755/j01.ms.19.3.2320

Received 30 August 2012; accepted 05 January 2013

A series of pure and copper-doped cobalt oxide films was prepared by plasma-enhanced metalorganic chemical vapor deposition (PEMOCVD). The effect of Cu-doping on the chemical structure and morphology of the deposited films was investigated. Raman and FTIR spectroscopies were used to characterize the chemical structure and morphology of the produced films. The bulk composition and homogeneity of the samples were investigated by energy dispersive X-ray microanalysis (EDX), and X-ray photoelectron spectroscopy (XPS) was employed to assess the surface chemical composition of pure and doped materials. The obtained results permit to affirm that the PEMOCVD technique is a simple, versatile and efficient method for providing homogeneous layers of cobalt oxides with a different content of copper. It has been found that pure cobalt oxide films mainly contain Co_3O_4 in the form of nanoclusters whereas the films doped with Cu are much more complex, and CoO_x (also Co_3O_4), mixed Co-Cu oxides and CuO_x nanoclusters are detected in them. Preliminary catalytical tests show that Cu-doped cobalt oxide films allow to initiate catalytic combustion of n-hexane at a lower temperature compared to the pure cobalt oxide (Co_3O_4) films. From what has been stated above, the plasma-deposited thin films of Cu-doped cobalt oxides pave the way towards a new class of nanomaterials with interesting catalytic properties.

Keywords: plasma deposition; copper-doped cobalt oxide catalysts; Raman spectroscopy; X-ray photoelectron spectroscopy; energy dispersive X-ray microanalysis.

1. INTRODUCTION

Transition metal oxides represent a group of very promising materials, which due to their properties can be used in extensive applications as gas sensors, coatings, solar absorbers, electrodes in supercapacitors, electrochromic devices and magnetic materials [1 – 6]. In recent years, much effort has been devoted to the use of these materials in catalysis [7 – 12]. Such extensive studies are related to the search for active, low cost replacements for noble metals (Pt, Pd, Rh), which show specific high activity but are costly, sensitive to poisoning and sintering [13 – 15]. Especially, various mixed transition metal oxides with the spinel structure, such as $NiFe_2O_4$ [16], $CuMn_2O_4$ [17], $CuCr_2O_4$ [18], $Cr_xCo_{3-x}O_4$ [19], $Li_xCo_{3-x}O_4$ [20], have been found very attractive in this field. Catalytic activity and performance of these materials have been remarkably improved, compared to non-doped materials, due to the interaction (synergetic effects) between different metal oxides dispersed on the surface [21 – 23].

Recently, much attention has been paid to copper-doped cobalt oxide nanocatalysts due to their ability to catalyze many important reactions including oxidation of CO [24], higher alcohol synthesis [25], NO reduction by CO [26], VOC combustion [27], methanol decomposition [28]. Several authors have described different methods of preparation of this type of catalytic materials including thermal decomposition, spray pyrolysis, sol-gel technique, chemical coprecipitation [29 – 32]. However, there are only a few reports concerning the plasma-enhanced chemical vapor deposition (PECVD), a method used to manufacture doped or mixed functional materials [33 – 37]. Itoh et al. [33] reported that the microwave plasma assisting CVD is a very convenient tool to obtain mixed oxide thin films from volatile β-diketonates as precursors. Arockiasamy et al. [35] described the synthesis of composite coatings Ni/TiO_2 by plasma-assisted metal-organic (PAMO) CVD using argon and nitrogen as discharge gases. Another example of the use of plasma enhanced CVD to produce glucose sensor are given by Seo et al. [37]. In this case, oxygen RF plasma, 150 W of power, was used to prepare Pd-doped tin oxide thin films from stannic chloride ($SnCl_4$) and palladium hexafluroacetylacetonate ($Pd(C_5HF_6O_2)_2$) as precursors.

As it was shown earlier, also by us [7, 38], the so-called "plasma catalysts" represent a group of materials exhibiting a high activity and catalytic efficiency comparable to or even better than "classical catalysts". Moreover, they allow for the reduction of production costs as well as environmental pollution. A utilized method (PEMOCVD) enables the control of grain size of nanocrystals [39], which attracted remarkable attention in different reactions sensitive to shape and crystal plane effects.

*Corresponding author. Tel.: +48-42-6313723, fax: +48-42-6313677.
E-mail address: *jatyczko@wipos.p.lodz.pl* (J. Tyczkowski)

Therefore, we make an attempt to manufacture copper-doped cobalt oxide nanocatalysts which may play a significant role in the chemical industry. Preliminary catalytical tests, carried out on the first batch of these catalysts, show that the initiation temperature of catalytic combustion of n-hexane is lower (220 ºC) and activation energy (111kJ/mol) is comparable to the pure cobalt oxide (Co_3O_4) nanocatalysts [27]. This encouraged us to continue the work on the optimization of plasma processes in order to achieve an uniform layer of copper-doped cobalt oxide nanocatalysts with different contents of copper in the composition.

The present work aimed to investigate the effect of Cu-doping on the chemical structure and morphology by Raman and FTIR spectroscopies. Energy dispersive X-ray microanalysis (EDX) and X-ray photoelectron spectroscopy (XPS) were employed to determine the bulk composition and homogeneity of the samples and the surface chemical composition of pure and doped materials, respectively.

2. EXPERIMENTAL PART

2.1. Deposition technology

The plasma-enhanced metalorganic chemical vapor deposition (PEMOCVD) was applied to produce copper-doped cobalt oxide films. A RF plasma reactor (13.56 MHz), which was used for deposition, is schematically shown in Fig. 1. A detailed description of the reactor was given elsewhere [40]. However, some changes have been made in the form of additional reservoir for liquid monomer with a separate system of temperature stabilization. To produce the films, bis(acetylacetonate) copper(II) ($Cu(acac)_2$ (Sigma-Aldrich 98 %), blue powder under standard condition with vapor pressure 6.65 Pa at 78 ºC, and cyclopentadienyl (dicarbonyl)-cobalt(I) ($CpCo(CO)_2$ (Stream Chemicals, Inc. min. 95 %), liquid under standard conditions, were used as precursors. Argon (99.999 % purity) and oxygen (99.95 % purity) were applied as the carrier gases with the flow 0.71 sccm and 0.1 sccm, respectively, regulated by Brook's mass flow controllers. The total pressure in the reactor chamber was approx. 4 Pa depending on the deposition parameters. The flow rate of $Cu(acac)_2$ was regulated by the change of the sublimation temperature with a fixed flow of $CpCo(CO)_2$ amounting to ca. 0.02 sccm. The glow discharge power was 40 W. The details of the preparation conditions are included in Table 1.

As substrates, glass plates with an evaporated thick Au layer (for Raman spectroscopy and ellipsometric measurements) and a thin gold foil (for EDX and XPS analysis) were used. For FTIR spectroscopy the films were deposited on thin (1 mm thick) pellets with a diameter of 13 mm obtained from cesium iodide (CsI Alfa Aesar, 99.9 %) using a hand forming press with the load of 1.7 GPa.

One of the type of samples (CoCu130Ar) was also modified by thermal treatment. In this case CoCu130ArW samples were produced. The treatment process was performed in a stream of air at the temperature of 350 ºC for 15 min.

2.2. Characterization techniques

To characterize the composition and homogeneity of the pure and doped materials, scanning electron microscopy with energy dispersive X-ray microanalysis (SEM-EDX FEI Quanta 200F with Oxford Instruments detector X-Max50) were used.

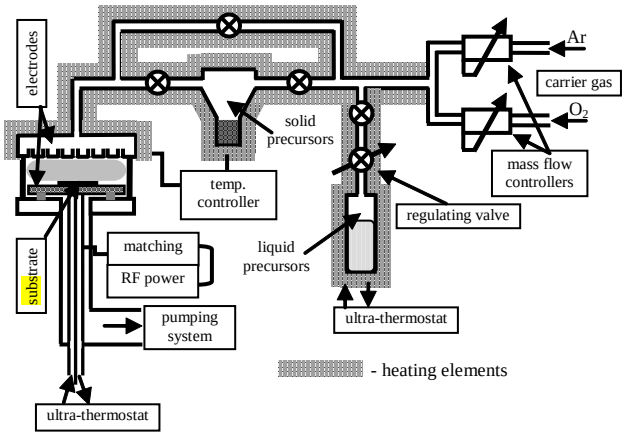

Fig. 1. A schematic diagram of RF plasma reactor.

The thickness of the pure copper oxide and pure cobalt oxide films was measured by a null ellipsometer Rudolf 431A working at an incident light wave of 632.8 nm.

The chemical structure and morphology of the films was investigated by FTIR and Raman spectroscopy. Fourier transform infrared transmission spectra (FTIR) were taken with Jasco FT/IR-6200 spectrometer with a spectral resolution of 0.5 cm^{-1} for MIR region 4000 cm^{-1} to 600 cm^{-1}. Raman spectra were obtained by a Jobin Yvon Raman spectrometer T64000, equipped with a microscope. As a source of light, an argon laser (λ = 514.5 nm) was used. All measurements were taken at the room temperature with integration time for every single spectrum equal to 15 min.

To assess the surface chemical composition of pure and doped materials, X-ray photoelectron spectroscopy (XPS) was employed. Photoelectron spectra were recorded on a Thermo VG ESCALAB 250 spectrometer equipped with a monochromatic Al K_α X-ray source (150 W, 15 kV,

Table 1. Preparation conditions of the samples

Sample name	Precursors	Carrier gas	Pressure [Pa]	Deposition time [min]	Thermal treatment
$CoArO_2$	$CpCo(CO)_2$ – 24 ºC	Ar + O_2	4.4	90	No
$Cu150ArO_2$	$Cu(acac)_2$ – 150ºC	Ar + O_2	4.4	90	No
CoCu130Ar	$CpCo(CO)_2$ – 24 ºC; $Cu(acac)_2$ – 130 ºC	Ar	4.0	60	No
CoCu130ArW	$CpCo(CO)_2$ – 24 ºC; $Cu(acac)_2$ – 130 ºC	Ar	4.0	60	Yes
$CoCu130ArO_2$	$CpCo(CO)_2$ – 24 ºC; $Cu(acac)_2$ – 130 ºC	Ar + O_2	4.6	90	No

1486.6 eV) at a spot size 500 µm, and a magnetic lens that makes it possible to obtain higher sensitivity. Base pressure in the analysis chamber was ca. 5×10^{-9} mbar; pass energy was set at 100 eV and 40 eV, with step size 1.1 eV and 0.11 eV for the survey and the narrow regions, respectively. Binding energies were determined by attributing to the main C1s peak a value of 284.9 eV. Sample charge compensation wasn't applied due to high content of carbon in the films and thus good conductivity. The obtained spectra have been processed involving background subtraction (Shirley-type), and a curve fittings procedure (mixed Gaussian 70 % – Lorentzian 30 % lines shape). The surface composition (at.%) was determined by considering the integrated peak areas and the corresponding atomic sensitivity factors.

3. RESULTS AND DISCUSSION

Ellipsometric studies provide us with information about the thickness of the investigated layers and their growth rate. However, only for pure materials it was possible to carry out measurements and determination of mentioned parameters. Unfortunately, for doped materials, this technique was insufficient to obtain accurate values of the thickness. For the mixture of Ar and O_2 as carrier gases, for pure materials we deposited films ($CoArO_2$; $Cu150ArO_2$) with thickness ~60 nm and growth rate ca. 0.67 nm/min. In all cases, the thickness of the films as a function of deposition time was linear.

To find in which way Cu-doping affected the chemical structure and morphology of the deposited films, Raman spectroscopy has been applied. Two evident regions of bands can be distinguished: the region I between 150 cm^{-1} and 800 cm^{-1} attributed to Co and Cu oxide structures, and the region II at $(1000-3500)$ cm^{-1} assigned to carbon structures (Fig. 2). As it can be seen in Fig. 2, A, some apparent Raman bands are observed in the region I for samples deposited with the mixture of Ar and O_2. For sample $CoArO_2$, the peaks are at 682, 610, 513, 471 cm^{-1} and 191 cm^{-1}, which originate from Co_3O_4 and had been reported previously [38]. Two characteristic bands exist for sample $Cu150ArO_2$, at 625 cm^{-1} and 445 cm^{-1}, which can be assigned to CuO_x. After comparing these bands with the database [41], we specified that we can have mixed CuO and Cu_2O oxides. This conclusion comes from the fact that the band at 625 cm^{-1} may originate from CuO or Cu_2O and the band at 440 cm^{-1} is observed only for Cu_2O. The sample prepared from the mixture of copper and cobalt precursors showed four peaks. The Raman peak observed at 682 cm^{-1} was assigned to A_{1g} modes of crystalline Co_3O_4, the band located at 445 cm^{-1} was recognized as belonging to Cu_2O. The two broad bands at 510 cm^{-1} and 615 cm^{-1} are not assigned and probably emerged as a result of mixed cobalt and copper oxides. As it can be seen in Fig. 2, B, for the sample prepared with Ar as a carrier gas, no apparent Raman bands are observed in the region 200 cm^{-1} to 800 cm^{-1}. It suggests that we have an amorphous structure with a very high dispersion of copper and cobalt oxides [38]. In the carbon region, three distinct bands were observed corresponding to the typical graphite G line centered at around 1560 cm^{-1} and the so-called disordered graphite D line centered around 1370 cm^{-1}, the third peak located at ca. 2950 cm^{-1} is associated with C–H bonds. Moreover, after thermal treatment, the situation was reversed because in the region II no bands were recognized, but in the region I several peaks appeared which correspond to the cobalt and copper oxides described above. Sample $CoCu130ArO_2$ shows bands in both regions of Raman spectra. However, the peaks in the carbon region are two times less intensive with comparison to those for sample CoCu130Ar. The difference stems from the addition of oxygen to the reaction mixture, which degrades the carbon structure. It is worth noting that such an addition of oxygen in the case of non-doped layers deposition is sufficient to completely remove the carbon structure.

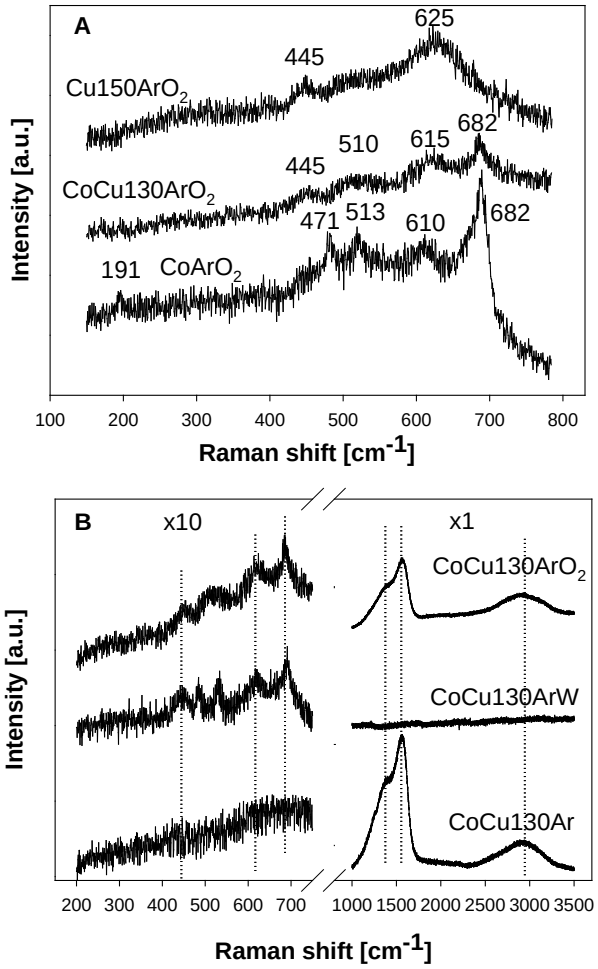

Fig. 2. Raman spectra of the investigated films: A – deposited with the mixture of Ar and O_2; B – copper-doped cobalt oxide films

For more information on the chemical structure of deposited films, FTIR spectroscopy was used. Typical spectra collected for pure and doped materials deposited in the mixture of Ar and O_2 are displayed in Fig. 3. The spectra suggest that these films, regardless of the type of deposited film, have in their structure an organic matrix rich in carbon bonded to hydrogen and oxygen. Being more precise, it should be stressed that the presented spectra show some very characteristic absorption bands: the strong bands centered at about 3450 cm^{-1} are assigned to the stretching vibration of O–H groups. Bands appearing at 2920 cm^{-1} and 2860 cm^{-1} are referred to asymmetric and symmetric stretching

vibration of CH_2, respectively. At 2950 cm^{-1}, there is a band originating from methyl groups. The band situated at 1100 cm^{-1} can be identified with C–O stretching vibrations. Bands from the range 1300 cm^{-1} – 1900 cm^{-1} are connected also with the organic matrix and suggest that its structure is quite complicated.

Based on the FTIR spectra we are not able to state clearly the presence of cobalt and copper oxides bands [30, 42, 43]. This problem will be further investigated, but already now we should emphasize the usefulness of Raman spectroscopy for the study of such oxide structures.

EDX analysis was used to find bulk composition of deposited films. The measurements were performed at ten different points to confirm the homogeneity of the layers. The results are shown in Table 2 together with the results obtained from XPS measurements for the surface chemical composition.

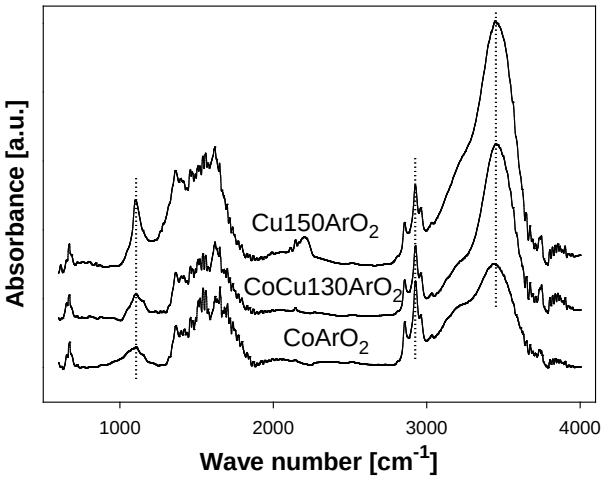

Fig. 3. FTIR spectra of the pure and doped materials deposited with mixed Ar and O_2 as carrier gas

As one can see, the presented results confirm the results from Raman and FTIR spectroscopy, proving the presence of carbon, oxygen, cobalt and copper in all samples. The observed significant differences between the bulk and surface composition could not be explained without an additional extensive study, and will be reported elsewhere. Such differences were already shown for films formed from mixtures of pure metal oxides [44, 45]. This was explained by surface segregation effects. In our case, however, the problem is much more complex due to the presence of the organic matrix which is in permanent interaction with the oxide fractions.

The XPS spectroscopy was used, apart from the determination of the surface composition, to identify the chemical structure of the pure and doped materials. Fig. presents the Core Level spectra of $Cu2p_{3/2}$, $Co2p_{3/2}$, O1s and C1s, while the binding energies values for cobalt and copper are compiled in Table 3. The fitted spectra of CoCu130Ar sample are displayed in Fig. 4 (C-I and D-I). In this case, cobalt exists in two chemical states on the surface, as Co^0 and Co^{2+}, with a satellite at higher binding energy, while copper appears only in one chemical state Cu^+ (or Cu^0) without any satellite. After thermal treatment, significant changes are observed on the surface (Fig. 4 (C-II and D-II)). Cobalt is no longer in a metallic form but it appears in the Co^{3+} state with a significant reduction in the content of Co^{2+} and simultaneous decreasing the intensity of the satellite peak. Copper is also changed and it occurs in two chemical states, as Cu^+ and Cu^{2+}, with an associated satellite peak. Similar results are obtained for $CoCu130ArO_2$ (Fig. 4 (C-III and D-III)), with slight differences in the intensities of individual peaks.

To proceed the comparative analysis, the $Cu2p_{3/2}$ and $Co2p_{3/2}$ spectra are shown in Fig. 4. A for pure materials deposited in the mixture of Ar and O_2. It should be stressed that the presence of a strong satellite peak for $Co2p_{3/2}$ indicates the presence of Co^{2+} on the surface with very little participation of Co^{3+}. Copper presents a very weak satellite peak, which points to a significantly higher concentration of Cu^+ on the surface with a small amount of Cu^{2+}. The representative spectra of C1s and O1s for a sample $CoCu130ArO_2$ are presented in Fig. 4, B. The O1s peak can be fitted by two components at 530.1 eV and 531.6 eV assigned to the O^{2-} anions of the crystalline network [46] and hydroxides, respectively. The C1s spectra were decomposed on three peaks at 284.9, 285.6 and 288.6 eV assigned to carbon chemical bonds occurring in the organic matrix existing in the samples.

Based on the above results, it can be concluded that for samples CoCu130Ar, CoCu130ArW, and $CoCu130ArO_2$ observed binding energies for $Co2p_{3/2}$ and $Cu2p_{3/2}$ agreed closely with literature [47, 48]. However, for pure materials (samples $CoArO_2$ and $Cu150ArO_2$) these bands are shifted by approx. 1 eV to higher and lower binding energies, respectively. The observed shifts can be connected with a strong interaction between two different oxide states occurring on the surface or may stem from particle size effects. In the case of cobalt, there is Co^{2+} and a small amount of Co^{3+} [49] whereas for copper, Cu^+ and a small concentration of Cu^{2+} occur [48, 50]. The O1s and C1s spectra are in close agreement with the results obtained from Raman and FTIR spectroscopy, and provide information about a chemical state of carbon and oxygen in deposited films.

Table 2. Composition of deposited films obtained by EDX analysis and XPS spectroscopy

Sample name	EDX				XPS			
	Co (at.%)	Cu (at.%)	C (at.%)	O (at.%)	Co (at.%)	Cu (at.%)	C (at.%)	O (at.%)
$CoArO_2$	26.69	–	25.88	47.43	15.69	–	41.83	42.48
$Cu150ArO_2$	–	16.39	29.99	53.62	–	15.41	53.93	30.67
CoCu130Ar	16.80	0.82	75.82	6.56	4.89	1.24	84.22	9.65
CoCu130ArW	30.93	1.41	26.74	40.92	22.57	1.54	25.31	50.58
$CoCu130ArO_2$	10.60	2.14	43.95	43.30	12.20	2.28	61.46	24.06

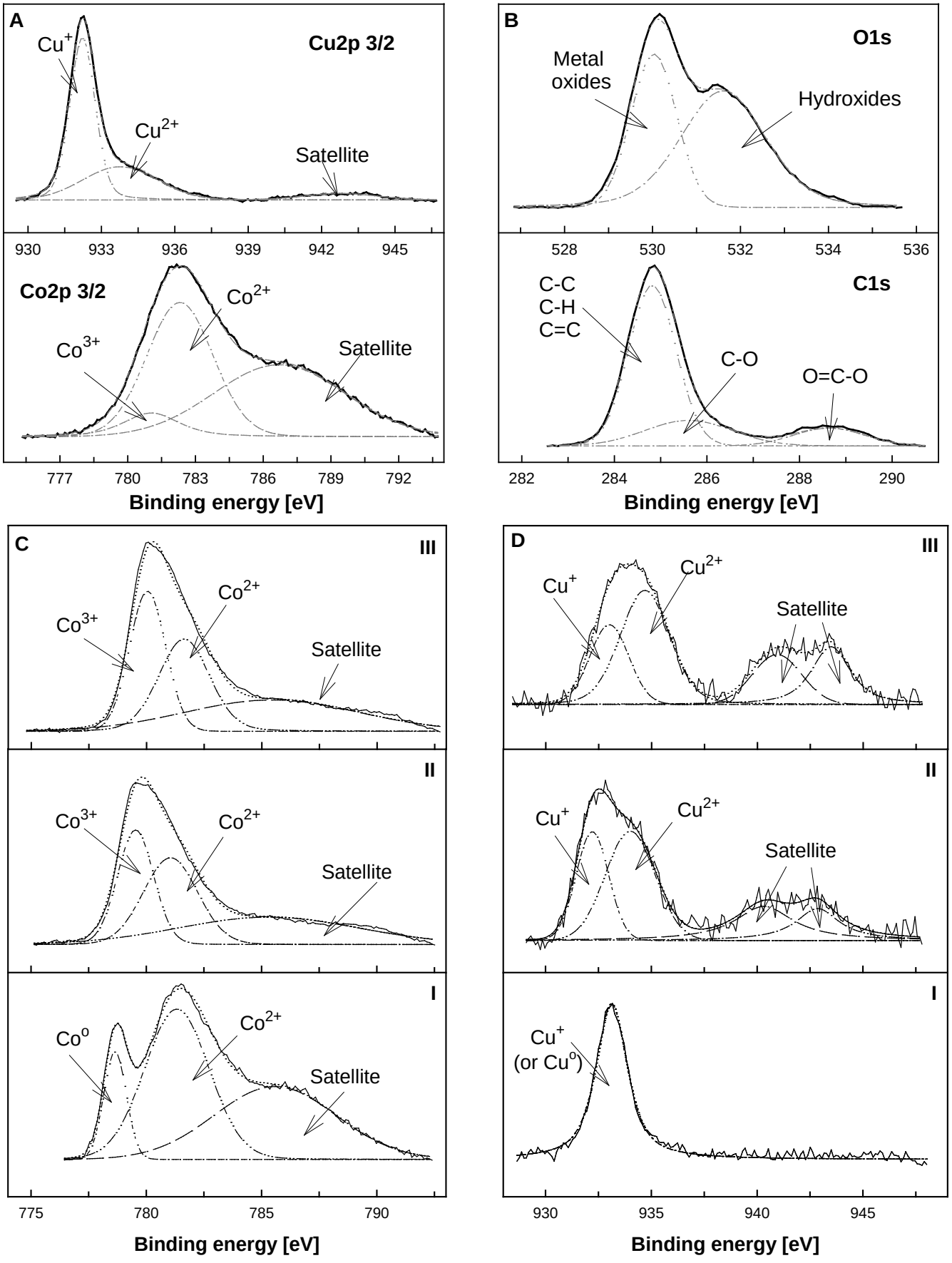

Fig. 4. Curve fittings of XPS spectra: A – $Co2p_{3/2}$ and $Cu2p_{3/2}$ spectra of a samples $CoArO_2$ and $Cu150ArO_2$ (non-doped samples); B – representative spectra of C1s and O1s of a sample $CoCu130ArO_2$ (doped samples); C – $Co2p_{3/2}$ for doped samples I – CoCu130Ar; II – CoCu130ArW; III – $CoCu130ArO_2$; D – $Cu2p_{3/2}$ for doped samples I – CoCu130Ar; II – CoCu130ArW; III – $CoCu130ArO_2$

Table 3. Binding energies for the Core Levels $Co2p_{3/2}$ and $Cu2p_{3/2}$ peaks of investigated samples

Sample name	$Co2p_{3/2}$				$Cu2p_{3/2}$			
	Binding energy [eV]				Binding energy [eV]			
	Co^0	Co^{2+}	Co^{3+}	Satellite	Cu^+(or Cu^0)	Cu^{2+}	Satellite	Satellite
$CoArO_2$	–	782.3	781.1	786.7	–			
$Cu150ArO_2$	–				932.3	933.7	942.8	
CoCu130Ar	778.7	781.3	–	785.6	933.2	–	–	–
CoCu130ArW	–	781.1	779.5	785.3	933.0	934.0	940.3	942.8
$CoCu130ArO_2$	–	781.6	780.1	785.5	933.1	934.7	941.0	943.5

4. CONCLUSIONS

The PEMOCVD method has proved to be a very useful technique for the preparation of copper-doped cobalt oxides thin films during the same plasma process. Depending on deposition parameters, films with different composition and chemical states of Co and Cu were obtained. It was found that typical spinel structure (Co_3O_4), especially interesting from the catalysis point of view, can be created in the films. Two forms of Cu atoms, namely Cu^+ and Cu^{2+}, were also distinguished. Unfortunately, it has failed to clearly demonstrate the presence of spinel structure type $Cu_xCo_{3-x}O_4$. Further research will be conducted in the direction of obtaining such a spinel structure in the plasma deposition process. Optimization of the catalytic properties of the copper-doped cobalt oxide films will also be carried out.

Acknowledgments

This work was supported by the Polish Ministry of Science and Higher Education, which funded the project No N209144736 (2009 – 2012). The financial support is gratefully appreciated. The authors wish to thank Dr. Philippe Decorse for his assistance with XPS measurements.

REFERENCES

1. **Aroutiounian, V.** Review. Metal Oxide Hydrogen, Oxygen, and Carbon Monoxide Sensors for Hydrogen Setups and Cells *International Journal of Hydrogen Energy* 32 2007: pp. 1145 – 1158.
2. **Gulbiński, W., Suszko, T., Sienicki, W., Warcholiński, B.** Tribological Properties of Silver- and Copper-doped Transition Metal Oxide Coatings *Wear* 254 2003: pp. 129 – 135.
3. **Avila, A. G., Barrera, E. C., Huerta, L. A., Muhl, S.** Cobalt Oxide Films for Solar Selective Surfaces, Obtained by Spray Pyrolysis *Solar Energy Materials & Solar Cells* 82 2004: pp. 269 – 278.
4. **Shinomiya, T., Gupta, V., Miura, N.** Effects of Electrochemical-deposition Method and Microstructure on the Capacitive Characteristics of Nano-sized Manganese Oxide *Electrochimica* Acta 51 2006: pp. 4412 – 4419.
5. **Gesheva, K. A., Ivanova, T., Hamelmann, F.** Optical Coatings of CVD-transition Metal Oxides as Functional Layers in "SMART WINDOWS" and X-ray Mirrors *Journal of Optoelectronics and Advanced Materials* 7 2005: pp. 1243 – 1252.
6. **Marco, J. F., Gancedo, J. R., Gracia, M., Gautier, J. L., Rios, E. I., Palmer, H. M., Greaves, C., Berry, F. J.** Cation Distribution and Magnetic Structure of the Ferromagnetic Spinel $NiCo_2O_4$ *Journals of Materials Chemistry* 11 2001: pp. 3087 – 3093.
7. **Łojewska, J., Kołodziej, A., Łojewski, T., Kapica, R., Tyczkowski, J.** Cobalt Catalyst Deposited on Metallic Microstructures for VOC Combustion: Preparation by Non-equilibrium Plasma *Catalysis Communications* 10 2008: pp. 142 – 145. http://dx.doi.org/10.1016/j.catcom.2008.07.042
8. **Bahlawane, N.** Kinetics of Methane Combustion over CVD-made Cobalt Oxide Catalysts *Applied Catalysis B: Environmental* 67 2006: pp. 168 – 176. http://dx.doi.org/10.1016/j.apcatb.2006.03.024
9. **Hu, Y., Dong, L., Wang, J., Ding, W., Chen, Y.** Activities of Supported Copper Oxide Catalysts in the NO+CO Reaction at Low Temperatures *Journal of Molecular Catalysis A: Chemical* 162 2000: pp. 307 – 316.
10. **Infantes-Molina, A., Merida-Robles, J., Rodriguez-Castellon, E., Fierro, J. L. G., Jimenez-Lopez, A.** Synthesis, Characterization and Catalytic Activity of Ruthenium-doped Cobalt Catalysts *Applied Catalysis A: General* 341 2008: pp. 35 – 42. http://dx.doi.org/10.1016/j.apcata.2007.12.034
11. **Pasha, N., Lingaiah, N., Seshu Babu, N., Siva Sankar Reddy, P., Sai Prasad, P. S.** Studies on Cesium Doped Cobalt Oxide Catalysts for Direct N_2O Decomposition in the Presence of Oxygen and Steam *Catalysis Communications* 10 2008: pp. 132 – 136.
12. **Haneda, M., Kintaichi, Y., Bion, N., Hamada, H.** Alkali Metal-doped Kobalt Oxide Catalysts for NO Decomposition *Applied Catalysis B: Environmental* 46 2003: pp. 473 – 482. http://dx.doi.org/10.1016/S0926-3373(03)00287-X
13. **Li, W. B., Wang, J. X., Gong, H.** Catalytic Combustion of VOCs on Non-noble Metal Catalysts *Catalysis Today* 148 2009: pp. 81 – 87. http://dx.doi.org/10.1016/j.cattod.2009.03.007
14. **Zhang, L., Zhang, J., Wilkinson, D. P., Wang, H.** Progress in Preparation of Non-noble Electrocatalysts for PEM Fuel Cell Reaction *Journal of Power Sources* 156 2006: pp. 171 – 182. http://dx.doi.org/10.1016/j.jpowsour.2005.05.069
15. **Lahousse, C., Bernier, A., Grange, P., Delmon, B., Papaefthimiou, P., Ioannides, T., Verykios, X.** Evaluation of γ-MnO_2 as a VOC Removal Catalyst: Comparison with a Noble Metal Catalyst *Journal of Catalysis* 178 1998: pp. 214 – 225.
16. **Santos, P. T. A., Costa, A. C. F. M., Kiminami, R. H. G. A., Andrade, H. M. C., Lira, H. L., Gama, L.** Synthesis of a $NiFe_2O_4$ Catalyst for the Preferential Oxidation of Carbon Monoxide (PROX) *Journal of Alloys and Compounds* 483 2009: pp. 399 – 401. http://dx.doi.org/10.1016/j.jallcom.2008.08.116
17. **Hosseini, S. A., Niaei, A., Salari, D., Nabavi, S. R.** Nanocrystalline AMn_2O_4 (A = Co, Ni, Cu) Spinels for Remediation of Volatile Organic Compounds-synthesis, Characterization and Catalytic Performance *Ceramics International* 38 2012: pp. 1655 – 1661. http://dx.doi.org/10.1016/j.ceramint.2011.09.057
18. **Boumaza, S., Bouarab, R., Trari, M., Bouguelia, A.** Hydrogen Photo-evolution over the Spinel $CuCr_2O_4$ *Energy Conversion and Management* 50 2009: pp. 62 – 68. http://dx.doi.org/10.1016/j.enconman.2008.08.027
19. **Kim, K. J., Park, Y. R., Hyun, D. H., Lee, S. H.** Optical Properties of Normal Spinel $M_xCo_{3-x}O_4$ (M=CrandCu): Coexistence of Charge-transfer and Crystal-field Transitions *Journal of Applied Physics* 96 2004: pp. 1975 – 1978.
20. **Nikolov, I., Darkaoui, R., Zhecheva, E., Stoyanova, R., Dimitrov, N., Vitanov, T.** Electrocatalytic Activity of Spinel

Related Cobaltites $M_xCo_{3-x}O_4$ (M = Li, Ni, Cu) in the Oxygen Evolution Reaction *Journal of Electroanalytical Chemistry* 429 1997: pp. 157 – 168.

21. **Imamura, S., Tsuji, Y., Miyake, Y., Ito, T.** Cooperative Action of Palladium and Manganese(III) Oxide in the Oxidation of Carbon Monoxide *Journal of Catalysis* 151 1995: pp. 279 – 284.
22. **Liu, L., Chen, Y., Dong, L., Zhu, J., Wan, H., Liu, B., Zhao, B., Zhu, H., Sun, K., Dong, L., Chen, Y.** Investigation of the NO Removal by Co on CuO-CoO_x Binary Metal Oxides Supported on $Ce_{0.67}Zr_{0.33}O_2$ *Applied Catalysis B: Environmental* 90 2009: pp. 105 – 114. http://dx.doi.org/10.1016/j.apcatb.2009.02.021
23. **Ozkan, U. S., Watson, R. B.** The Structure-function Relationships in Selective Oxidation Reactions over Metal Oxides *Catalysis Today* 100 2005: pp. 101 – 114. http://dx.doi.org/10.1016/j.cattod.2004.12.018
24. **Wojciechowska, M., Przystajko, W., Zieliński, M.** CO Oxidation Catalysts Based on Copper and Manganese or Cobalt Oxides Supported on MgF2 and Al2O3 *Catalysis Today* 119 2007: pp. 338 – 341. http://dx.doi.org/10.1016/j.cattod.2006.08.035
25. **Hui-Yuan Xu, Wei Chu, Li-Min Shi, Hui Zhang, Si-Yu, Deng.** Effect of Glow Discharge Plasma on Copper-cobalt-aluminum Catalysts for Higher Alcohol Synthesis *Journal of Fuel Chemistry and Technology* 37 2009: pp. 212 – 216.
26. **Xia, C., Junfeng, Z., Yan, H., Zhiquan, T., Ming, H.** Catalytic Reduction Of Nitric Oxide with Carbon Monoxide on Copper-cobalt Oxides Supported on Nano-titanium Dioxide *Journal of Environmental Science* 21 2009: pp. 1296 – 1301.
27. **Łojewska, J., Kołodziej, A., Kapica, R., Knapik, A., Tyczkowski, J.** In Search for Active Non-precious Metal Catalyst for VOC Combustion. Evaluation of Plasma Deposited Co and Co/Cu Oxide Catalysts on Metallic Structured Carriers *Catalysis Today* 147S 2009: pp. S94 – S98.
28. **Marban, G., Lopez, A., Lopez, I., Valdes-Solis, T.** A highly Active, Selective and Stable Copper/cobalt-structured Nanocatalysts for Methanol Decomposition *Applied Catalysis B: Environmental* 99 2010: pp. 257 – 264.
29. **La Rosa-Toro, A., Berenguer, R., Quijada, C., Montilla, F., Morallon, E., Vazquez, J. L.** Preparation and Characterization of Copper-doped Cobalt Oxide Electrodes *The Journal of Physical Chemistry B* 110 2006: pp. 24021 – 24029.
30. **Gautier, J. L., Trollund, E., Rios, E., Nkeng, P., Poillerat, G.** Characterization of Thin $CuCo_2O_4$ Films Prepared by Chemical Spray Pyrolysis. Study of Their Electrochemical Stability by Ex situ Spectroscopic Analysis *Journal of Electroanalytical Chemistry* 428 1997: pp. 47 – 56. http://dx.doi.org/10.1016/S0022-0728(96)05072-3
31. **Singh, R. N., Pandey, J. P., Singh, N. K., Lal, B., Chartier, P., Koenig, J.-F.** Sol-gel Derived Spinel $M_xCo_{3-x}O_4$ (M = Ni, Cu; $0 \le x \le 1$) Films and Oxygen Evolution *Electrochimica Acta* 45 2000: pp. 1911 – 1919. http://dx.doi.org/10.1016/S0013-4686(99)00413-2
32. **Fierro, G., Lo Jacono, M., Inversi, M., Dragone, R., Porta, P.** TPR and XPS Study of Cobalt-copper Mixed Oxide Catalysts: Evidence of a Strong Co-Cu Interaction *Topics in Catalysis* 10 2000: pp. 39 – 48. http://dx.doi.org/10.1023/A:1019151731177
33. **Itoh, K.-I., Matsumoto, O.** Deposition Process of Metal Oxide Thin Films by Means of Plasma CVD with β-diketonates as Precursors *Thin Solid Films* 345 1999: pp. 29 – 33.
34. **Martin, A., Espinos, J. P., Justo, A., Holgado, J. P., Yubero, F., Gonzalez-Elipe, A. R.** Preparation of Transparent and Conductive Al-doped ZnO Thin Films by ECR Plasma Enhanced CVD *Surface and Coatings Technology* 151 – 152 2002: pp. 289 – 293.
35. **Arockiasamy, S., Raghunathan, V. S., Premkumar, P. A., Kuppusami, P., Dasgupta, A., Parameswaran, P., Mallika, C., Nagaraja, K. S.** Plasma-assisted MOCVD of Titanium Oxide and Its Composite Coatings Using Metallo-organic Precursors *Chemical Vapor Deposition* 13 2007: pp. 691 – 697.
36. **Tyczkowski, J., Delamar, M.** Ultraviolet Luminescence of Gd-doped a-$Si_XC_YO_Z$:H Films Fabricated by Plasma Chemical Vapor Deposition *Materials Science and Engineering B* 146 2008: pp. 151 – 156.
37. **Seo, H.-K., Ansari, S. G., Al-Deyab, S. S., Ansari, Z. A.** Glucose Sensing Characteristics of Pd-doped Tin Oxide Thin Films Deposited by Plasma Enhanced CVD *Sensors and Actuators B: Chemical* 168 2012: pp. 149 – 155. http://dx.doi.org/10.1016/j.snb.2012.03.078
38. **Tyczkowski, J., Kapica, R., Łojewska, J.** Thin Cobalt Oxide Films for Catalysis Deposited by Plasma-enhanced Metal-organic Chemical Vapor Deposition *Thin Solid Films* 515 2007: pp. 6590 – 6595.
39. **Tyczkowski, J.** New Materials for Innovative Energy Systems Produced by Cold Plasma Technique *Functional Materials Letters* 4 2011: pp. 341 – 344.
40. **Kapica, R., Redzynia, W., Tyczkowski, J.** Characterization of Palladium-based Thin Films Prepared by Plasma-enhanced Metalorganic Chemical Vapor Deposition *Materials Science* (*Medžiagotyra*) 18 2012: pp. 128 – 131.
41. Raman Spectra Database of Minerals and Inorganic Materials RASMIN Web http://riodb.ibase.aist.go.jp/rasmin/
42. **Lenglet, M., Lefez, B.** Infrared Optical Properties of Cobalt(II) Spinels *Solid State Communications* 98 1996: pp. 689 – 694. http://dx.doi.org/10.1016/0038-1098(96)00109-3
43. **Lefez, B., Souchet, R., Kartouni, K., Lenglet, M.** Infrared Reflection Study of CuO in Thin Oxide Films *Thin Solid Films* 268 1995: pp. 45 – 48. http://dx.doi.org/10.1016/0040-6090(95)06872-4
44. **Langell, M. A., Gevrey, F., Nydegger, M. W.** Surface Composition of $Mn_xCo_{1-x}O$ Solid Solution by X-ray Photoelectron and Auger Spectroscopies *Applied Surface Science* 153 2000: pp. 114 – 127.
45. **Pyke, D., Mallick, K. K., Reynolds, R., Bhattacharya, A. K.** Surface and Bulk Phases in Substituted Cobalt Oxide Spinels *Journal of Materials Chemistry* 8 1998: pp. 1095 – 1098.
46. **Dupin, J.-C., Gonbeau, D., Vinatier, P., Levasseur, A.** Systematic XPS Studies Of Metal Oxides, Hydroxides and Peroxides *Physical Chemistry Chemical Physics* 2 2000: pp. 1319 – 1324. http://dx.doi.org/10.1039/a908800h
47. **Petitto, S. C., Marsh, E. M., Carson, G. A., Langell, M. A.** Cobalt Oxide Surface Chemistry: The Interaction of CoO(100), Co_3O_4(110) and Co_3O_4(111) with Oxygen and Water *Journal of Molecular Catalysis A: Chemical* 281 2008: pp. 49 – 58.
48. **Dong, L., Zhang, L., Sun, C., Yu, W., Zhu, J., Liu, L., Liu, B., Hu, Y., Gao, F., Dong, L., Chen, Y.** Study of the Properties of $CuO/VO_x/Ti_{0.5}Sn_{0.5}O_2$ Catalysts and Their Activities in NO + CO Reaction *ACS Catalysis* 1 2011: pp. 468 – 480.
49. **Fernandez-Garcia, M., Martinez-Arias, A., Hanson, J. C., Rodriguez, J. A.** Nanostructured Oxides in Chemistry: Characterization and Properties *Chemical Reviews* 104 2004: pp. 4063 – 4104.
50. **Papavasiliou, J., Avgouropoulos, G., Ioannides, T.** Combined Steam Reforming of Methanol over Cu–Mn Spinel Oxide Catalysts *Journal of Catalysis* 251 2007: pp. 7 – 20. http://dx.doi.org/10.1016/j.jcat.2007.07.025